Turk J Phys
27 (2003) , 537 – 549.

Structural, Electrical and Spectral Studies on Double Rare-Earth Orthoferrites $La_{1-x}Nd_xFeO_3$

Osama Mohamed HEMEDA, Mohsen Mohamed BARAKAT,
Dalal Mohamed HEMEDA
Physics Department, Faculty of Science, Tanta University-EGYPT
e-mail: mbarakato@yahoo.com

Received 24.02.2003

Abstract

Samples of double rare-earth ferrite $La_{1-x}Nd_xFeO_3$ are synthesized by a high-temperature double sintering ceramic technique. X-ray diffraction shows that all compounds have an orthorhombic structure. The values of lattice parameter and the volume of the unit cell, changes with increasing Nd^{3+} content. The Goldschmidt tolerance factor decreases and goes far from unity with increasing Nd content. The samples containing Nd ions with $x = 0.1$, 0.2 and 0.3 have higher resistivity than that of $LaFeO_3$, but for x ≥ 0.4 the resistivity decreases. The results indicate the presence of extrinsic semiconducting properties up to 100 °C above which the hopping conduction appears. Thermoelectric power measurements show that the main charge carriers are electrons. The decrease of the Seebeck coefficient and the concentration of charge carrier in the region above 100 °C, indicates the weakening of the hopping conduction mechanism. The samples were characterized for pyroelectric voltage and IR absorption spectra.

Key Words: Orthoferrite, X-ray, Electrical properties, IR.

1. Introduction

The largest number of $A^3B^3O_3$ type compounds has been found by Geller and Wood [1], and have an orthorhombic structure, similar to that of $GdFeO_3$. The space group for these compounds is Pbnm. The relationship of the orthorhombic unit cell to that of the perovskite structure has been studied earlier. $GdFeO_3$ has the unit cell structure

$a = 5.346$ Å,$b = 5.616$ Å and $c = 7.665$ Å and contains four distorted perovskite units. It is quite possible that many $A^3B^3O_3$ compounds, which have been reported to have monoclinic structure, could in reality have orthorhombic structure. In the pervoskite structure, the A cation is coordinated with twelve oxygen ions, and the B cation with six. Thus the A cation is normally found to be somewhat larger than the B cation. The requirements for stability of the pervoskite structure are: the B ion should have a preference for octahedral arrangement and the anion should fit into the cavity formed by the corners of the shared BO_6 octahedra. Orthoferrite have the general formula RFO_3 where R is a large trivalent metal ion, such as a rare earth or an Y ion. They crystallize in a distorted perovskite structure with an orthorhombic unit cell [2]. The orthoferrite forms of La and Y are isostructural and belong to the Pbnm space group [1]. They have the following lattice parameters:

$LaFeO_3$ a = 5.556 Å b = 5.65 Å c = 7.862 Å at $T_c = 738$ K

$YFeO_3$ a = 5.302 Å b = 5.587 Å c = 7.622 Å at T_c = 643 K

In both $LaFeO_3$ and $YFeO_3$, each Fe^{3+} is surrounded by 6 antiparallels Fe^{3+} nearest- neighbors, according to neutron diffraction data [3, 4]. The weak ferromagnetism in the orthoferrite is due to antisymmetric exchange interaction [5]. Magnetic studies have shown that in several orthoferrites the canting is governed by an antisymmetric exchange mechanism [6]. In most orthoferrites the rare earth ions are paramagnetic (at sufficiently high temperature) and give an approximate contribution to the magnetic susceptibility of the material. The magnetic structure of the magnetic moment in the orthoferrite can be visualized as a system of two sublattices strongly coupled antiferro-magnetically and slightly canted by perturbing interaction to produce a net ferromagnetic moment perpendicular to the anti-ferromagnetic axis [7].

It was reported that the electrical conduction in $LaFeO_3$ can be attributed to the hopping conduction mechanism and the deviation from unity in La/Fe greatly affects the conductivity [8]. The distorted perovskites $RFeO_3$ (R being rare earth or Y) called rare earth orthoferrites are known for a rich variety of interactions between the rare earth and Fe ions and for the number of magnetic phase transitions that occur in them. These canted antiferromagnets crystallize in the D_{2n}^{16} Pbnm space group with $RFeO_3$ molecules per unit cell (four Fe^{3+} ions and four rare-earth ions per unit cell). Just below the Neel temperature (between 600−800 K) depending on the rare earth, the iron spin subsystem is ordered according to the $\Gamma_4(G_xA_yF_z)$representation of the space group, while the rare earth ion moment are paramagnetic and polarized in a configuration belonging to the same mode $\Gamma_4(f_z)$. We follow the notation of Bertaut [9] and the common practice of using G, F, A and C as basis vector to describe the Fe^{3+} spin system and corresponding lower letters to describe the rare earth system. Physically this means that Fe^{3+} spins are ordered antiferromagnetically along the orthorhombic axis a, with a small canting of the ab plane which produces a weak ferromagnetic moment Falong the C-axis. The canting is generally very small so that the magnitude of the antiferromagnetic vector G is usually much larger than that of the ferromagnetic moment F and the weak antiferromagnetic moment A and G. If we neglect the canting, G is parallel to Fe^{3+} spins. The interaction between Fe^{3+} and R^{3+} ions are anisotropic and temperature dependent. Macroscopically it means a gradual change of directions of the weak ferromagnetism from c to a axis upon cooling. Microscopically, the Fe^{3+} spins and G rotate continuously from a to c is over a temperature range of several K. The beginning and end of this reorientation are each marked by a second order phase transition [10]. The final magnetic state is described as $\Gamma_2(F_x\,C_y\,G_z\,,\ f_x\,c_y)$. The intermediate magnetic configuration is described as $\Gamma_{24}$by Yamaguchi and Tsushim [11] and is sometimes referred to as an angular phase. $La\,Nd\,Fe\,O_3$ is one of the orthoferrites where a spin reorientation takes place according to $\Gamma_4 - \Gamma_{24} - \Gamma_2$ pattern. The Neel temperature of $NdFeO_3$ is (T_N = 760 K) [12]. Below it the magnetic ordering of Fe^{3+} ions is that of a canted antiferromagnetic of the G-type. At room temperature the net moments $F$of Fe^{3+} ions lie along the C axis whereas the sublattice moment G lie in (a, b) plane being slightly canted to the a axis [13].

1.1. Experimental procedure

A series of $La_{1-x}Nd_xFeO_3$ samples were prepared by the double sintering ceramic technique, where x = 0, 0.1, 0.2, 0.3, 0.4 and 0.5. The oxides were ground in an agate mortar for 10 hrs to ensure homogeneity. The mixtures were presintered at 900 °C for 2 hrs and gradually cooled to room temperature. The powder was ground again and pressed as tablets and finally sintered at 1250 °C for 6 hrs.

The samples we examined under x-ray diffraction using a Philips model PW-1729 diffractometer and Cu-K_α radiation.

The DC resistivity was measured using a Keithely 610 C electrometer at various temperatures. The IR absorption spectra of the given samples were recorded using Perkin Elmer 1430 IR spectrophotometer.

The Seebeck coefficient α (thermoelectric power) was measured using an apparatus given elsewhere [14].The sample is tightly pressed between two copper electrodes by means of load placed on top of it. Each electrode is attached to a thermocouple and connection wires .The lower surface of the sample is attached

to an internal heater to keep the temperature gradient across the sample surfaces during measurements. External heater was used to keep a constant temperature around the sample. An evacuated metal jacket cooled with water was placed around the apparatus.

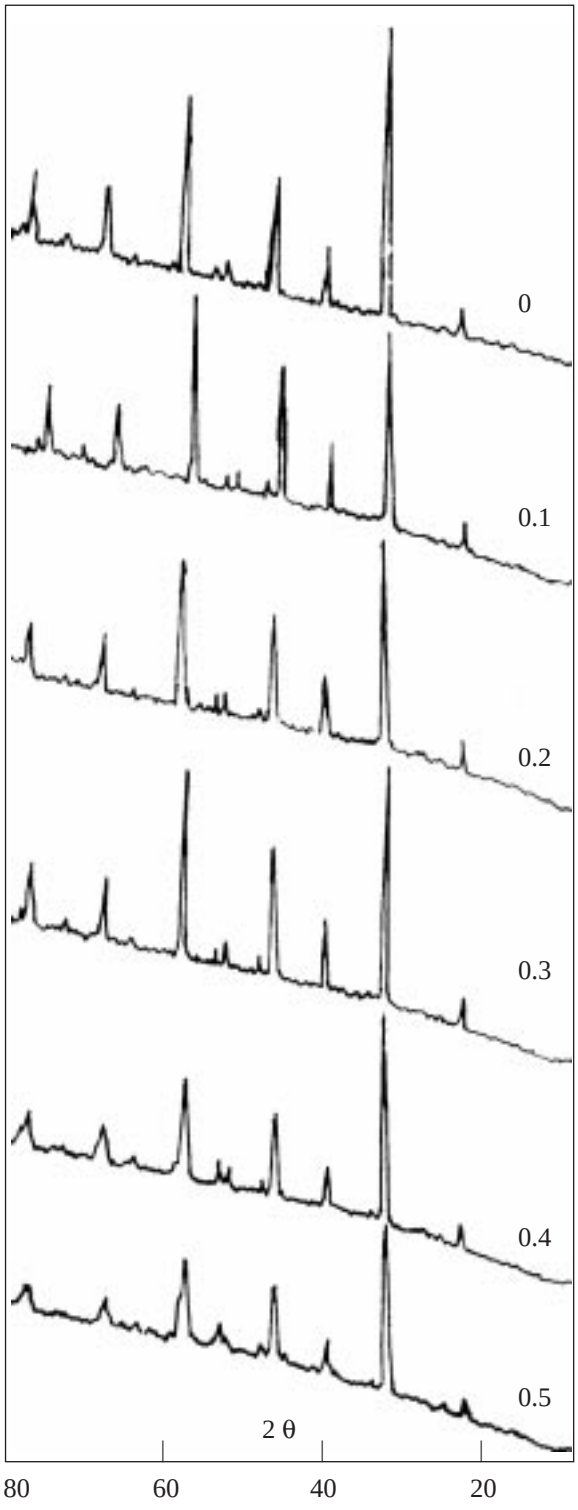

Figure 1. The Cu-Kα x-ray diffraction pattern of $La_{1-x}Nd_xFeO_3$ (where x = 0, 0.1, 0.2, 0.3, 0.4 and 0.5).

2. Results and discussion

2.1. X-ray analysis

The X-ray diffraction analysis of $La_{1-x}Nd_xFeO_3$ indicates that all the samples possess an orthorhombic structure. The calculated lattice parameters a, b and $c$and unit cell volume are listed in Table 1. The results indicate that the structure of the compounds is similar to that of $RFeO_3$ as reported by Geller and Wood [1].

Figure 1 shows the Cu- K_α x-ray diffraction patterns of La_{1-x} Nd_x FeO_3 for $x = 0$, 0.1, 0.2, 0.3, 0.4 and 0.5. Because of the difference between the radius of the R ions and the Fe ions, the structure of $RFeO_3$ is not ideal perovskite, and the Fe^{3+} ions and O^{2-} ions depart from the ideal positions. In $La_{1-x}Nd_x$ FeO_3 the distortion will be larger because there are two kinds of ions, La and the second rare earth ion at the R sites. In accordance with literature data, the material belongs to the orthoferrite crystal system [1].Table I shows derived x-ray data, including the unit cell parameters a, b, c, and the volume of the unit cell. The larger ions occupy the A positions, which is coordinated with twelve oxygen ions, and the smaller ions occupy the B sites, which is coordinated by six. Accordingly the La ions occupy the A positions and Fe^{3+} occupy B sites. The requirement for stability of this orthoferrite is that the Goldschmidt tolerance factor t should be of nearly unity[16] where t is defined via

$$R_A + R_O = t\sqrt{2}(R_B + R_O),$$

where R_A, R_B and R_O are radii of A, B sites and oxygen ion respectively.

Table 1. The lattice parameters, tolerance factor, and R_A, R_B radii as a function of Nd content.

X	Compound	a, Å	b, Å	c, Å	V, (Å^3)	t	R_A	R_B
0	$LaFeO_3$	5.51	5.62	7.81	241.8	0.887	1.14	0.64
0.1	$La_{0.9}Nd_{0.1}FeO_3$	5.59	5.62	7.12	223.86	0.883	1.13	0.64
0.2	$La_{0.8}Nd_{0.2}FeO_3$	5.63	5.59	7.08	222.66	0.880	1.12	0.64
0.3	$La_{0.7}Nd_{0.3}FeO_3$	5.63	5.59	7.07	222.67	0.876	1.11	0.64
0.4	$La_{0.6}Nd_{0.4}FeO_3$	5.64	5.59	7.07	222.90	0.873	1.1	0.64
0.5	$La_{0.5}Nd_{0.5}FeO_3$	5.73	5.59	6.96	222.70	0.869	1.09	0.64

From the table the values of a and b are approximately equal $c/\sqrt{2}$. The volume of the unit cell decreases with increasing the Nd content because the radius of $Nd^{3+} = 0.109$ Å is smaller than $La^{3+} = 0.114$ Å. The values of lattice parameter a, b, c and the volume of the unit cell are near that of $LaFeO_3$, which has the values $a = 5.53$ Å, $b = 5.57$Å, $c = 7.8$ Å and $v = 241$ Å^3. The tolerance factor as shown in Table 1, decreases and ranges far from unity, indicating that the lattices are distorted by increasing the Nd content. When Nd is substituted for La, the lattice is distorted slightly by the smaller Nd ion and both the orthorhombic unit cell volume and the c axis became smaller. The substitution of Nd for La may cause c/a to decrease, as shown in Figure 2. The replacement of La by Nd at A sites may reduce the covalent bond formation by La ions, thereby decreasing the lattice parameter c and increase a. Figure 3 shows the bulk and theoretical density as a function of Nd content x. The theoretical density is estimated by the empirical equation$D_x = \frac{3M}{NV}$, where M is the sample molecular weight and V is its volume. The density of the samples generally increases with increasing Nd content. The theoretical density D_x is greater than the bulk density due to the presence of pores in the materials. The orthorhombic phase obstructs the movement of grain boundaries and prevents the exaggerated grain growth resulting in smaller grains with a reduced number of inner pores leading to the increase of density.

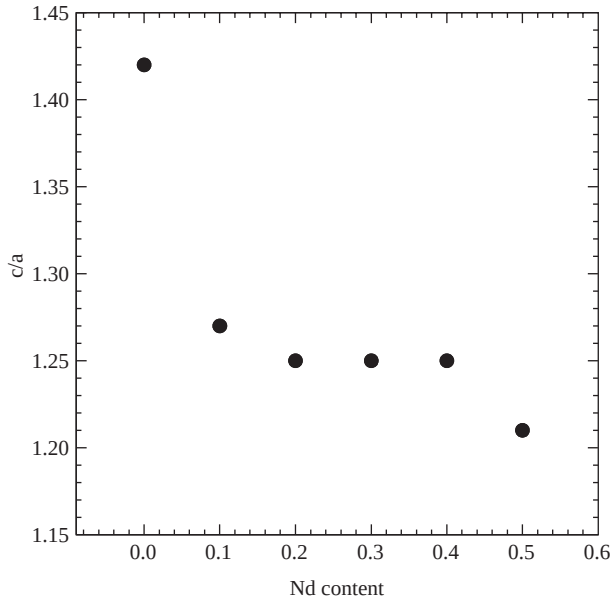

Figure 2. The ratio of lattice parameters c/a as a function of Nd content.

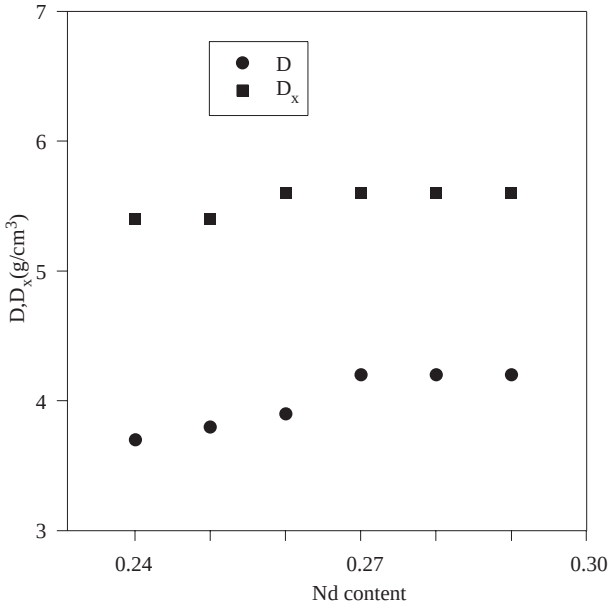

Figure 3. The bulk and theoretical densities as a function of Nd content.

2.2. Electrical properties

It is known that the rare-earth oxides are good electrical insulators and have resistivity at room temperature greater than $10^6\Omega$.cm [15]. All rare earth ions increase the electrical resistivity of orthoferrite, as the result of the formation of an insulating intergrainual phase $RFeO_3$. Figure 4 shows a plot of $\ln\rho$ as a function of inverse temperature for the samples of $La_{1-x}Nd_xFeO_3$; and shows a consistent decrease of resistivity with increasing temperature. Also, one can distinguish two regions of different activation energies except for $x = 0.4$ and 0.5. The change in the slope of these lines takes place around $T_a = 120$ °C. All the curves can be described by the equation

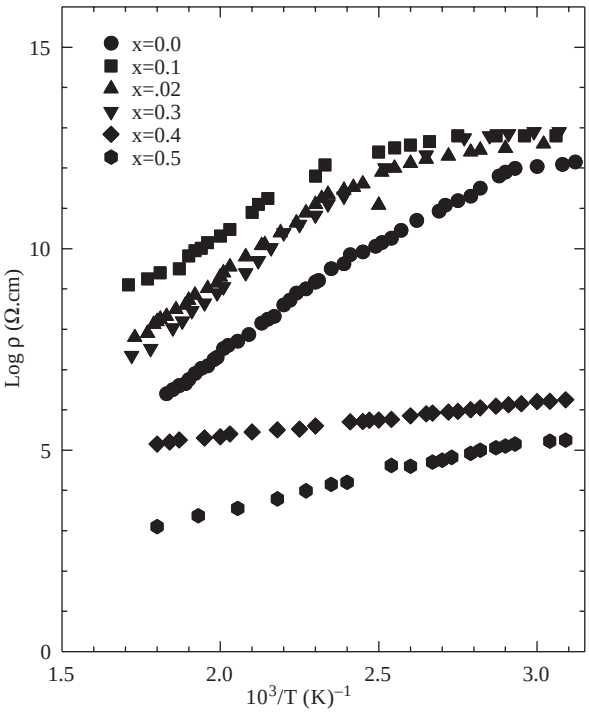

Figure 4. The relation between log ρ and 10^3/T, for $La_{1-x}Nd_xFeO_3$ (x = 0.0, 0.1, 0.2) (x = 0.3, 0.4 and 0.5).

$$\rho = A_1 \exp(E_1/kT) + A_2 \exp(E_2/kT),$$

Where E_1 and E_2 are the activation energies, below and above T_a respectively.

The samples containing Nd with x = 0.1, 0.2 and 0.3 have higher resistivity than that of $LaFeO_3$. For $x \geq 0.4$, the resistivity decreases again, possibly because the presence of the orthorhombic phase forms the distorted pervoskite unit cell. At $x \geq 0.4$, the generation of Nd^{4+} ions (from Nd^{3+} ions at sintering temperatures above 1250 °C), with their small radius, can substitute for Fe^{3+} , generating Fe^{2+} ions at B positions that will participate in the conduction process and decrease the resistivity.

Table 2. Electrical data

Nd content	Activation energy, ev		Δ E, eV	T_a, °C
	Below T_a	Above T_a		
$x = 0$	0.75	1.078	0.330	129
$x = 01$	0.40	0.863	0.462	110
$x = 0.2$	0.48	0.916	0.436	108
$x = 0.3$	0.22	1.078	0.863	105
$x = 0.4$	0.23	-	-	-
$x = 0.5$	0.14	-	-	-

Table 2 gives the activation energies in the two regions as a function of Nd content. The region below T_a = 120 °C is characterized by a low activation energy for all samples, which strongly suggests the conduction mechanism in the ferrite is a form of electron hopping between Fe^{3+} and Fe^{2+} ions at octahedral sites. In this first temperature interval the activation energies varies from 0.14 to 0.75 eV. The jump in the activation energy $\Delta E = E_2 - E_1$ was obtained for all samples. The ΔE jump is larger for higher Nd content. The steeper slopes of the straight lines at higher temperatures can be regarded as due to thermally activated

mobility of charge carriers and not to a thermally activated generation of these carriers. This would provide a simple explanation for the high conductivity at high temperatures. The resistivity decreases gradually from room temperature to 80 °C with an abrupt change at about 120 °C due to the transition from extrinsic to hopping conduction mechanism. It is evident to note that the abrupt change in log ρ vs 10^3/T has its highest value for $LaFeO_3$ (T_a = 129 °C), and becomes small as Nd content increase for x = 0.1, 0.2 and 0.3 are 110 °C, 108 °C and 105 °C, respectively. This is significally attributed to the higher impurity content for the former as a result of Nd substitution. The introduction of Nd ion in the lattice affects the magnetic order and help the spin moment of Fe^{3+} to reorient at lower temperature. Thus the electrical conductivity of such orthoferrite could be caused by electron hopping and diffusion among Fe ions of variable vacancy state (situated in equivalent points of orthoferrite lattice).

The electrical resistivity at room temperature increases with increasing Nd content, as shown in Figure 5 up to x = 0.3. The lattice distortion increases with increasing Nd content, which has a smaller ionic radius than La^{3+}. As it is known, the Nd ions, which affect the distance between the magnetic ions Fe^{2+} and Fe^3, substitute for La^{3+} ions and promote the Fe^{3+} ions to migrate from B to A positions. Thus as the Nd ions occupy modified positions, the number of scattering centers will increase, leading to the increase of resistivity up to x = 0.3.

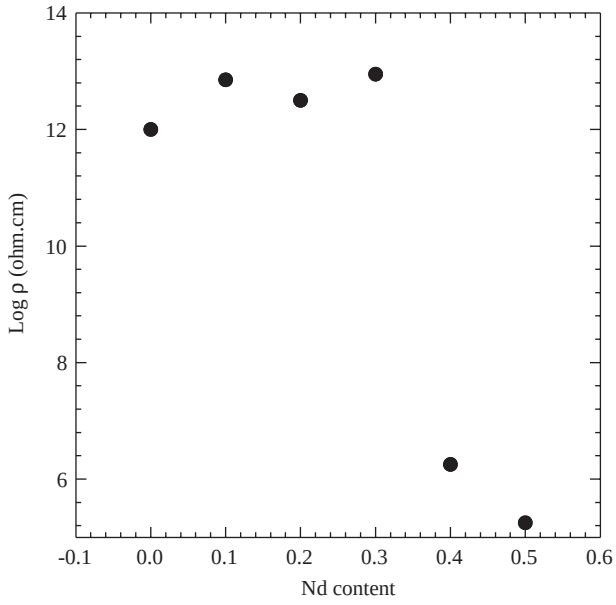

Figure 5. The resistivity of $La_{1-x}Nd_xFeO_3$ as a function of Nd content.

The effect of temperature on the mobility of charge carriers is shown in Figure 8, from which one may notice that the mobility increases with temperature to maximum value at 100 °C, then decreases temperatures above. This indicates the presence of two predominant conduction mechanisms: electrons hopping between Fe^{3+}, Fe^{2+} ions; and band conduction via the migration of La^{3+} ions from A to B sites increases the jump length of electrons at the B sites leading to reducing the mobility of electrons which are the majority carries in these compositions.

Thermoelectric power

In the case of hopping conduction the Seebeck coefficient is given by the relation $\alpha = \frac{2.3k}{e} \log\left(\frac{N_s}{n} - 1\right)$, where N_s is the average number of Fe^{3+}ions per unit volume and n is the number of charge carriers per unit volume. The mobility $\mu = \frac{1}{ne\rho}$ where ρ is the resistivity.

The Seebeck coefficient α as function of temperature is shown in Figure 6, and show negative values, indicating the presence of electronic conduction. The Seebeck coefficient increases with increasing temperature up to 100 °C and then decreases at higher temperatures. The behavior of α-T plots indicates that the number of charge carriers in these materials increase with temperature up to 100 °C and then decrease, for samples $x = 0.1$, $x = 0.3$, and $x = 0.5$ as shown in Figure 7.The other samples at $x = 0.2$ and 0.4 have the same behavior. This indicates the presence of two predominant conduction mechanisms, electron hopping between Fe^{2+} and Fe^{3+}at the octahedral coordination sites and band conduction. The increase of temperature increases the majority carriers (electrons) because the jump rate of the electrons depends on the temperature, leading to an increase in the thermoelectric power and the number of charge carriers as shown in Figure 7. The first region may be due to mainly an extremist band conduction [17]. Above 100 °C the decrease of charge carrier concentrations and the thermoelectric power may be due to the substitution of Fe^{3+} ions by La^{3+}ions at the B sites which decreases the number of Fe^{3+} ions at the octahedral coordination sites leading to a decrease in the hopping rate of electrons between Fe^{3+} and Fe^{2+}.

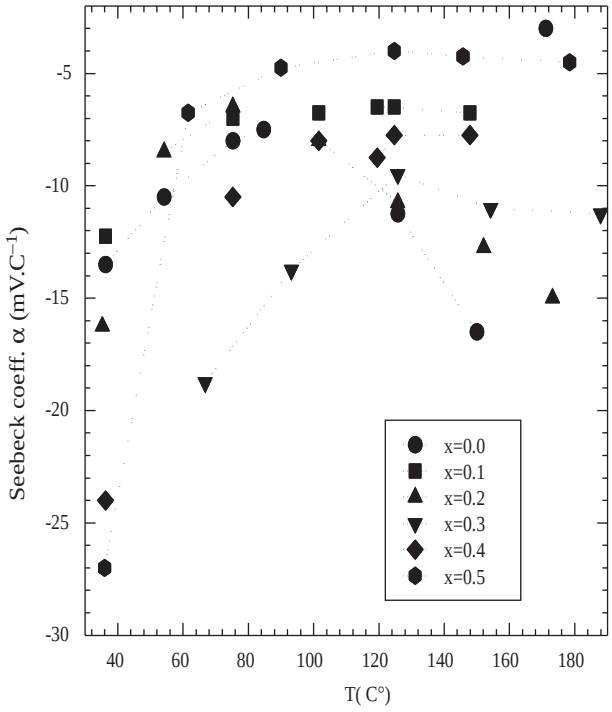

Figure 6. The Seebeck coefficient α as a function of temperature for all samples.

The presence of an extrinsic band conduction mechanism was confirmed from the behavior of the electrical resistivity versus temperature response of our samples. The mobility of charge carriers is thermally activated and increase rapidly with temperature up to 100 °C, then decrease, as shown in Figure 8. This indicates the presence of two predominant conduction mechanisms which involve hopping between Fe^{2+} and Fe^{3+} and due to impurity band conduction. The migration of La ions from A to B sites increases the jump length of electrons at B sites leading to reduction of the mobility of electrons with increasing Nd content.

2.3. The Pyroelectric Voltage

In the perovskite orthoferrite solid solution system, $Ba_{1-x}R_xFeO_3$ orthorhombic phases with space group (222) and pbn2 have been reported as crystals with composition having the latter polar symmetry. It is also evident that our system exhibits spontaneous magnetic moment, pyroelectricity and linear magneto- electric effects [18]. The pyroelectric coefficient is defined as the change in polarization per unit temperature change

of the specimen. Thus the pyroelectric effect is characterized by measuring the change in spontaneous polarization with the change in temperature. Figure 9 shows the variation of pyroelectric voltage with temperature. The alignment of domains to be parallel to the polar axis during heating takes place and contributes to the pyroelectricity. The substitution of Nd ions in the place of La ions contributes formation of the distorted prevoskite structure at the grain boundaries, which increase the resistivity and retard the carriers mobility, causing a decrease in pyroelectric voltage up to $x = 0.3$. At $x = 0.4$ and 0.5, the resistivity decreases and the electron hopping between Fe^{2+} and Fe^{3+} give a new contribution to the polarization, leading on increase of pyroelectric voltage.

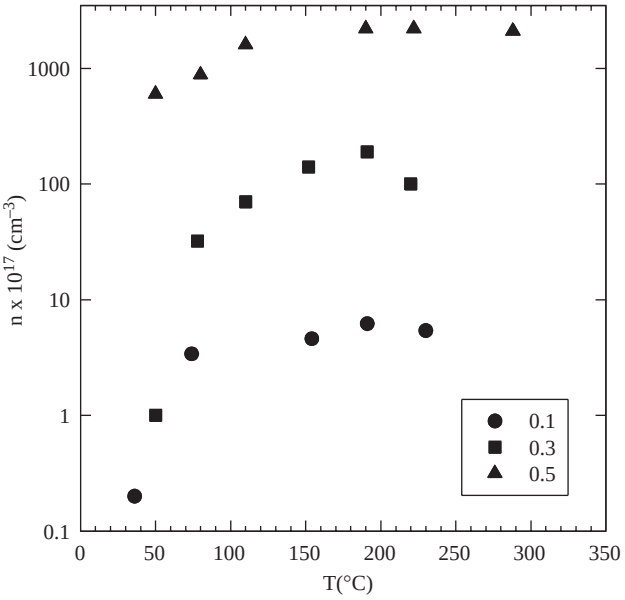

Figure 7. The concentration of charge carriers as a function of temperature.

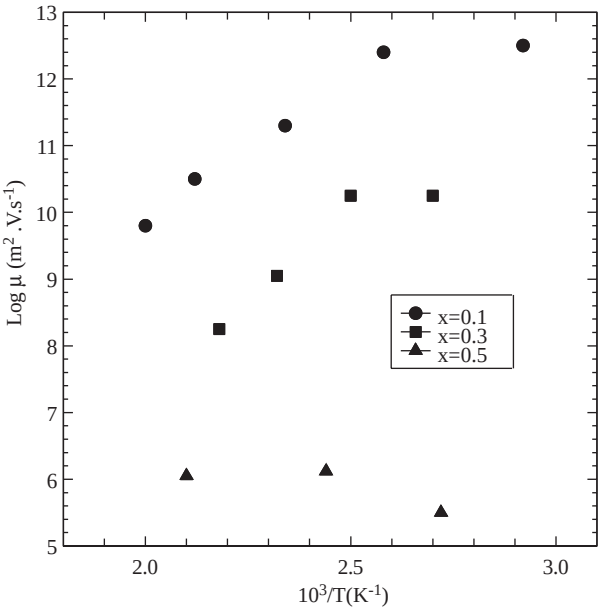

Figure 8. The mobilities of charge carriers as a function of temperature.

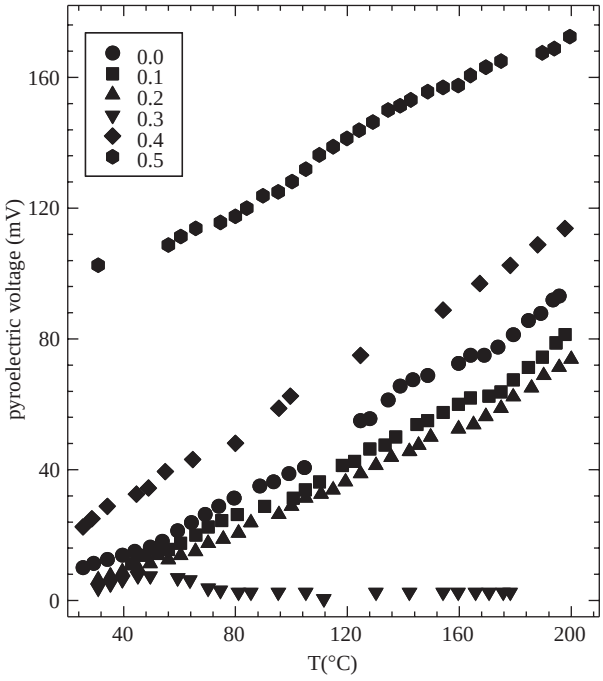

Figure 9. The pyroelectric voltage of $La_{1-x}Nd_xFeO_3$ as a function of temperature.

2.4. I. R. spectral analysis

I.R. absorption spectra of $La_{1-x}Nd_xFeO_3$ for (x = 0, 0.1, 0.2, 0.3, 0.4 and 0.5) were recorded as shown in Figure 10. It is clear that the I.R spectra of the given ferrite showed two characteristic absorption bands in the far infrared region. The lower frequency band assigned to oxygen octahedron and O-Fe-O bending vibration [19], whereas the higher frequency absorption band assigned to oxygen tetrahedral and Fe-O stretching vibration. The other weak bands appeared near lower frequency absorption band results from the oscillation of divalent metal ion-O bond [20]. The spectra of the entire ferrite sample have been used to locate the band positions and are given in Table 3.

The lower frequency absorption band ν_2 shifted to higher frequency as Nd content increases and ν_1 shifts to lower frequency. The broadening of the spectral band is due to statistical distribution of cations over A and B positions. The vibration frequency depends on the cation mass, cation-oxygen distance and bending force. The change in the lattice constant is responsible for this shift of the frequencies. The shift in ν_1 from 563 to 558 cm^{-1} is due to the change in balance of A ions positions, which probably causes the oxygen ions to shift towards the Nd^{3+} ions.

Table 3

Nd content	ν_1 cm^{-1}	I	ν_2 cm^{-1}	I	ν_3 cm^{-1}	I	ν_4 cm^{-1}	I	$\Gamma\nu_1$ dyn/cm	$\Gamma\nu_2$ dyn/cm
0.0	563	5.6	407	4.5	221	2.6	-	-	5.3×10^5	1.2×10^5
0.1	563	14.6	407	12.5	221	2.6	372	12.5	5.3×10^5	1.2×10^5
0.2	563	35.5	406	33.3	221	2.6	372	32.1	5.3×10^5	1.26×10^5
0.3	561	15.2	406	12	221	2.6	374	16.7	2.4×10^5	1.26×10^5
0.4	562	5	413	4.5	221	2.6	372	4.7	2.42×10^5	1.31×10^5
0.5	558	10.3	414	5.2	221	2.6	373	-	2.39×10^5	1.32×10^5

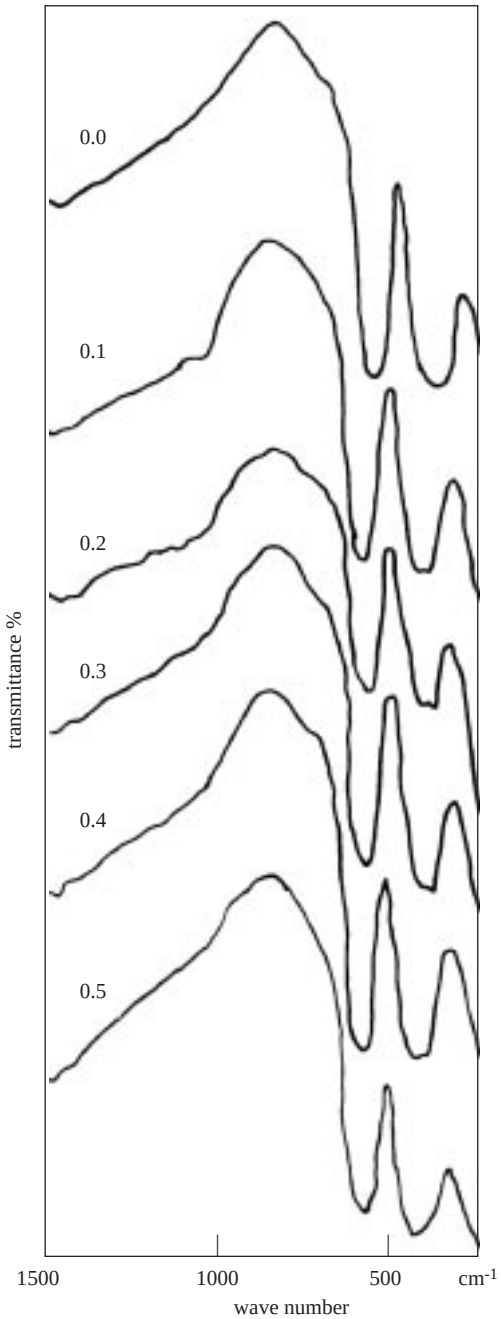

Figure 10. The infrared absorption spectra for $La_{1-x}Nd_xFeO_3$.

A splitting occurred at the ν_2 absorption band, which is assigned to the formation of Fe^{2+}, and confirm our discussion for explanation the mechanism of conduction at$x \geq 0.4$. It has been shown by potakova et al. [21], that the presence of Fe^{2+} ions at octahedral sites can produce splitting in the IR absorption bands. This is attributed to Jahn-Teller distortion produced by Fe^{2+} ions, which produce local deformation in the crystal field potential and hence lead to the splitting of the absorption band. The splitting appeared at 372 cm^{-1}. This band is assigned ν_4 and can be attributed to Fe^{2+}-O^{2-} vibration. The band ν_3 denotes to La^{3+}-O^{2-} bond vibrations. The shift for ν_2 occurred at high Nd content ($x = 0.4$ and 0.5). Also from the IR spectra it can be noticed that intensity of both two characteristic bands ν_1 and ν_2 increases as Nd content increases, up to $x = 0.2$, a then decrease. It is known that the intensity ratio is a function of the

change in dipole moment with intermolecular distance dμ/dr [20]. This value represent the contribution of Fe-O bond to the dipole moment, so the I.R. gives an idea about the change of molecular structure of ferrite due to change in Fe-O bonds by introducing Nd^{3+} ions. The difference in bonds positions of ν_1 and ν_2 is expected because of the difference in Fe^{3+}-O^{2-} distance for the octahedral and tetrahedral complexes. Since the frequency is proportional to the force constant, the ν_1 band shifts to lower frequency with increasing Nd ions indicates that the force constant decreases. The calculated value of force constant are given in Table 2 where$\Gamma = 4\pi^2 c^2 \nu^2 \mu$, where μ is the effective mass = $\frac{m_1 m_2}{m_1+m_2}$, in which m_1, m_2 are the mass of the Fe^{3+} and O ions, respectively.

There is a correlation between the structure and the geometry of the exchange bonds, specially the angle and length of the chemical bond Fe-O-Fe. Information about the unoccupied oxygen state in the rare-earth orthoferrite studied samples $LaNdFeO_3$ is necessary because of the important role that oxygen plays in the interaction between RE element and iron ions in these compounds. The strength of the indirect exchange interaction is characterized by the angle of interaction which has large value in $NdFeO_3$ = 151.3. The decrease in the bond angle Fe-O-Fe results in a weaker overlap between Fe3d and O2p shells and hence a small negative charge on the oxygen atom which reduce the oxygen energy level. On the other hand the electronic distributions of Fe-O bond is greatly affected when Nd ions with $4f^4 5d^6 6s^2$ orbitals is introduced in its neighborhood and thus consequently affects dμ/dr of the Fe-O bond leading to the change of the vibration frequencies, as shown by the IR absorption spectra.

3. Conclusion

The substitution of Nd ions in $LaFeO_3$ gives an orthoferrite system with lattice parameter in the range given in literature. The perovskite lattice was distorted by Nd substitution and the tolerance factor varies far from unity, causing the lattice parameters a, b to decrease and c to increase. The density increases with increasing Nd content because the formation of orthorhombic phase prevents grain growth and decrease the number of pores. The d.c. resistivity as a function of temperature showed that the samples of have two regions with different activation energies. The spin reorientation, or MI phase transition, occurs at temperature T_a and affect the conduction process. T_a shifts to lower temperature with increasing Nd content and disappears at $x = 0.4$ and 0.5. The measurement of thermoelectric power indicates that electrons are the majority carriers. The conduction mechanism can be described by the hopping model for samples $x = 0.1$, 0.3, 0.4 and 0.5 as suggested by the relatively constant relationship between α and T; but for samples with $x = 0.0$ and 0.2, the band conduction mechanism is predominant. The samples studied exhibit pyroelectric voltage indicating the presence of polar symmetry. The pyroelectric voltage, increases with increasing temperature and decreases with increasing Nd content up to $x = 0.4$, then rises. The IR spectra shows the presence of two absorption bands ν_1 and ν_2, corresponding to tetrahedral and octahedral group complexes. As the Nd content increases, the lower frequency band shifts to higher values and the higher frequency band shifts to lower frequency. The splitting at the absorption band ν_2 indicates the presence of divalent iron ions Fe^{2+}, which produce local deformation in the crystal field potential. The intensity of bands ν_1 and ν_2, increases with increasing Nd content, which is a function of intermolecular distance dμ/dr. The electronic distribution of Fe-O bond is greatly affected when Nd ions is introduced in its neighborhood and thus affect dμ/dr of the Fe-O bond, leading to the change of vibration frequency, as shown in the IR spectra.

References

[1] S. Geller and E. Wood, *Acta Cyst.*, **9**, (1956), 563.

[2] C. Rao, Solid State Chemistry. Marcel Dekker Inc. (1974) p.29,30,32,33,357,394.

[3] W. Koebler and E. Wallan, *J. Phys. Shem. Solids*, **2**, (1957), 100.

[4] W. Koebler, E. Wallan and M. Wilkinson, *Phys. Rev.,* **118**, (1960) 58.

[5] D. Treves, *J. Appl. Phys.*, **36**, (1965), 1033.

[6] D. Treves, *Phys. Rev. Vol.*, **125**, (1962), 1843.

[7] Plevy. I. Jacob, H. Uarne and L. Lewnson, *J. Appl.Phys.,* **42 (4),** (1971), 1631.

[8] S.A. Patil, S.M. Otari, V.C. Mahajan, M.G. Patil, M.K. Sovdagas, B.L. Patil and S.R. Swant, *Solid State Communications*, Vol. 78 No. 1, (1991), 39.

[9] E.F. Bertaut, (New York Academic) (1963), p 149.

[10] H. Horner and C.M. Varma, *Phys. Rev. Lett.*, **20**, (1958), 845.

[11] T. Yamaguchi and K. Tsushima, *Phys. Rev.*, **B8,** (1973) 5187.

[12] J.K. Vassiliou et al., *Solid State Chem.*, **81**, (1989), 208.

[13] J.B. Torrance et al., *Phys. Rev.,* **B45,14**, (1992), 8209.

[14] O.M. Hemeda et al., *J. Thermal Analysis,* **38**, (1992), 2291.

[15] E. Rezlescu, N. Rezlescu, P.D. Popa, L.Rezlescu and C. Pas, *Nicu. Phys. Stat. Sol. (a)* **162**, (1997), 673.

[16] V.M. Goldschmidt, *Naturwissenschaffen*, **14**, (1926), 477-485.

[17] B.L. Patil, S.R. Sawant, S.A. Patil, R.N. Patil, *J. of Material Science,* **29**, (1994), 175.

[18] I.C. Dwerus, O.G. Maln and A.W. Thomson, *Proc. Roy. Soc.*, **A275**, (1963), 295.

[19] K. Li, X. Li, K. Zhu, J. Zha and Y. Zhang, *J. Appl. Physics*, **81, 10**, (1997), 6943.

[20] C. Roa, Chem. Appl. Of IR Spec. "Academic press (1963), p.356.

[21] V.A. Patakova, N.D. Zverv and V.P. Romanov, *Phys. Stat. Sol.*, **12**, (1972), 623.